International Journal for Parasitology: Drugs and Drug Resistance 21 (2023) 40–50

Contents lists available at ScienceDirect

International Journal for Parasitology: Drugs and Drug Resistance

journal homepage: www.elsevier.com/locate/ijpddr

Effect of geranylated dihydrochalcone from *Artocarpus altilis* leaves extract on *Plasmodium falciparum* ultrastructural changes and mitochondrial malate: Quinone oxidoreductase

Agriana Rosmalina Hidayati [a,b], Melinda [c], Hilkatul Ilmi [d], Takaya Sakura [e,f], Miako Sakaguchi [g], Junko Ohmori [f], Endah Dwi Hartuti [c,h], Lidya Tumewu [d], Daniel Ken Inaoka [e,f,i], Mulyadi Tanjung [j], Eri Yoshida [e], Fuyuki Tokumasu [k], Kiyoshi Kita [f,i,l], Mihoko Mori [m], Kazuyuki Dobashi [m], Tomoyoshi Nozaki [i], Din Syafruddin [n], Achmad Fuad Hafid [d,o], Danang Waluyo [c], Aty Widyawaruyanti [d,o,*]

[a] *Doctoral Program, Faculty of Pharmacy, Universitas Airlangga, Surabaya, Indonesia*
[b] *Department of Pharmacy, Faculty of Medicine, Universitas Mataram, Mataram, Indonesia*
[c] *Research Center for Genetic Engineering, National Research and Innovation Agency (BRIN), Bogor, Indonesia*
[d] *Center of Natural Product Medicine Research and Development, Institute of Tropical Disease, Universitas Airlangga, Surabaya, Indonesia*
[e] *Department of Molecular Infection Dynamics, Institute of Tropical Medicine (NEKKEN), Nagasaki University, Nagasaki, Japan*
[f] *School of Tropical Medicine and Global Health, Nagasaki University, Nagasaki, Japan*
[g] *Central Laboratory, Institute of Tropical Medicine (NEKKEN), Nagasaki University, Nagasaki, Japan*
[h] *Graduate School of Biomedical Science, Nagasaki University, Nagasaki, Japan*
[i] *Department of Biomedical Chemistry, Graduate School of Medicine, The University of Tokyo, Bunkyo-ku, Japan*
[j] *Department of Chemistry, Faculty of Science and Technology, Universitas Airlangga, Surabaya, Indonesia*
[k] *Department of Cellular Architecture Studies, Institute of Tropical Medicine (NEKKEN), Nagasaki University, Nagasaki, Japan*
[l] *Department of Host-Defense Biochemistry, Institute of Tropical Medicine (NEKKEN), Nagasaki University, Nagasaki, Japan*
[m] *Kitasato Institute for Life Science, Kitasato University, Tokyo, Japan*
[n] *Department of Parasitology, Faculty of Medicine, Hasanudin University, Makassar, Indonesia*
[o] *Department of Pharmaceutical Sciences, Faculty of Pharmacy, Universitas Airlangga, Surabaya, Indonesia*

ARTICLE INFO

Keywords:
Geranylated dihydrochalcone
Artocarpus altilis
Plasmodium falciparum
Ultrastructural changes
*Pf*MQO

ABSTRACT

Nearly half of the world's population is at risk of being infected by *Plasmodium falciparum,* the pathogen of malaria. Increasing resistance to common antimalarial drugs has encouraged investigations to find compounds with different scaffolds. Extracts of *Artocarpus altilis* leaves have previously been reported to exhibit *in vitro* antimalarial activity against *P. falciparum* and *in vivo* activity against *P. berghei*. Despite these initial promising results, the active compound from *A. altilis* is yet to be identified. Here, we have identified 2-geranyl-2′, 4′, 3, 4-tetrahydroxy-dihydrochalcone (**1**) from *A. altilis* leaves as the active constituent of its antimalarial activity. Since natural chalcones have been reported to inhibit food vacuole and mitochondrial electron transport chain (ETC), the morphological changes in food vacuole and biochemical inhibition of ETC enzymes of (**1**) were investigated. In the presence of (**1**), intraerythrocytic asexual development was impaired, and according to the TEM analysis, this clearly affected the ultrastructure of food vacuoles. Amongst the ETC enzymes, (**1**) inhibited the mitochondrial malate: quinone oxidoreductase (*Pf*MQO), and no inhibition could be observed on dihydroorotate dehydrogenase (DHODH) as well as bc_1 complex activities. Our study suggests that (**1**) has a dual mechanism of action affecting the food vacuole and inhibition of *Pf*MQO-related pathways in mitochondria.

* Corresponding author. Center of Natural Product Medicine Research and Development, Institute of Tropical Disease, Universitas Airlangga, Surabaya, Indonesia.
E-mail address: aty-w@ff.unair.ac.id (A. Widyawaruyanti).

https://doi.org/10.1016/j.ijpddr.2022.12.001
Received 29 July 2022; Received in revised form 5 December 2022; Accepted 6 December 2022
Available online 8 December 2022

1. Introduction

Malaria is a parasitic disease caused by *Plasmodium falciparum* and transmitted through the female Anopheles mosquito bite. The World Malaria Report (2020) reported that in 2019, 229 million cases were estimated, with 409,000 deaths from malaria (WHO, 2020). Efforts are needed to identify and develop new antimalarials that are more effective, safer, have fewer side effects, are cheaper, and are easier to obtain than current drugs (Cui et al., 2015). The success of the plant-derived antimalarial drugs atovaquone, quinine, and artemisinin, highlights the importance of studying and exploring plants as sources of antimalarial agents. Between 2000 and 2017, 175 antiplasmodial compounds from plants were reported (Pan et al., 2018). Moreover, the ethnopharmacological approach has proved to be more beneficial for discovering new leads than robust random screening (Saxena et al., 2003).

The Moraceae family of plants consists of 60 genera that include 1,400 species (Somashekhar et al., 2013). The largest genus of the Moraceae family is *Artocarpus,* which contains 50 species. The greatest diversity of the Moraceae family is found in the western Malesian area. The species found within Malesia are distributed as follows: Peninsula Malaysia 16 species, Sumatra 17, Borneo 23, the Philippines 15, Sulawesi 6, Java 4, the Lesser Sunda Islands 3, the Moluccas 8, and New Guinea 6 (Lemmens et al., 1995). The extracts and metabolites of *Artocarpus*, especially leaves, barks, stems, and fruits, have been reported to contain phenolic compounds that are bioactive and used by the locals as traditional medicines (Jagtap and Bapat, 2010). Several *Artocarpus* studies have shown that extracts of the aerial and underground plant parts have been used for the treatment of diarrhea, diabetes, malarial fever, tapeworm infection, and other ailments (Balbach, 1992; Heyne and Jakarta, 1987; Perry, 1980). Other uses include wound healing, antisyphilic, expectorant, anti-anemia, asthma, and dermatitis (Hakim et al., 2006).

Flavonoids are secondary metabolites widely found in plants, and the antimalarial activity of this group has been reported (Saxena et al., 2003). Previous studies have shown that prenylflavonoids isolated from the stembark of *A. champeden* had antimalarial activity. Some of the active compounds isolated from this plant included: artocarpone A, artocarpone B, artoindonesianin E, heteroflavanone C, artoindonesianin R, heterophyllin, artoindonesianin A-2, cycloheterophyllin, and artonin A. Heteroflavanone C showed the most potent inhibition against *P. falciparum* growth with an IC_{50} value of 1 nM (Widyawaruyanti et al., 2007). A prenylated chalcone, isolated from *A. champeden* stem bark extract, namely morachalcone A, was also identified and can be used as a marker compound in the standardization of *A. champeden* stem bark ethanolic extract for antimalarial drug development (Hafid et al., 2012). Leaf and stembark extracts from other *Artocarpus* species, *A. altilis, A. heterophyllus,* and *A. camansi,* have also been reported to have effective antimalarial activity against *P. falciparum* and *P. berghei* (Hafid et al., 2016).

Extracts from *A. altilis* syn. *A. communis,* and *A. incises* (Kochummen, 1982; Verheij and Coronel, 1992), popularly known as breadfruit, have been reported to contain several bioactive compounds, such as morin, moracin, dihydromorin, cynomacurin, oxydihydroartocarpesin, artocarpetin, broussochalcone A, kazinol A, broussoaurone A, cycloartocarpin A, cycloheterophyllin, and broussoflavonol F (Akanbi et al., 2009; Sikarwar et al., 2014). A previous study demonstrated that the leaf extract from *A. altilis* could inhibit the growth of *P. falciparum in vitro* with an IC_{50} value of 1.32 μg/mL (Hafid et al., 2016). Furthermore, this extract was highly active against *P. berghei in vivo* with an ED_{50} value of 0.82 mg/kg body weight. Although the antimalarial activity of leaf extract from *A. altilis* has been previously demonstrated, its active compound has not been characterized.

Natural chalcones have previously been reported to inhibit the metabolic functions essential for parasite survival in food vacuole and mitochondria (Gomes et al., 2017; Takac et al., 2018). The food vacuole is a major digestive organelle of the malaria parasite and a validated chemotherapeutic target. This organelle plays an essential role in the degradation of erythrocyte-derived hemoglobin. It is the site of important classes of antimalarials, such as chloroquine, and harbors active transporters associated with drug resistance (Wunderlich et al., 2012). The mitochondrial electron transport chain (ETC) has been previously reported to be inhibited by chalcones (Mi-Ichi, 2005). *P. falciparum* ETC is composed of five dehydrogenases that are type-II NADH dehydrogenase (NDH2), succinate dehydrogenase (SDH), malate: quinone oxidoreductase (MQO), dihydroorotate dehydrogenase (DHODH), and glycerol-3-phosphate dehydrogenase (G3PDH). Each dehydrogenase transfers electrons from respective substrates to ubiquinone, producing ubiquinol. The electrons from ubiquinol are transferred ultimately to oxygen by a sequential reaction of quinol: cytochrome *c* reductase (bc_1 complex or complex III) and cytochrome *c* oxidase (complex IV), which are coupled with proton translocation across the inner membrane and the formation of electrochemical gradient which is used by ATP synthase (complex V) for production of ATP through oxidative phosphorylation (Hartuti et al., 2018). Amongst the ETC enzymes described above, DHODH, MQO, and bc_1 complex are known to be essential at the intraerythrocytic stage (Goodman et al., 2017; Hartuti et al., 2018; Niikura et al., 2017; Painter et al., 2007; Siregar et al., 2015; Wang et al., 2019). DHODH is the rate-limiting step in pyrimidine *de novo* biosynthesis and the target of DSM265, which showed promising results in Phase I and IIa clinical trials (Lianos-Cuentas et al., 2018; McCarthy et al., 2017). In *P. falciparum*, MQO has been proposed to be involved in the ETC, tricarboxylic acid (TCA), and fumarate cycles. The fumarate cycle seems required to provide cytosolic oxaloacetate, which is converted into aspartate to feed the purine salvage and pyrimidine *de novo* biosynthesis pathways (Hartuti et al., 2018; Niikura et al., 2017). *Plasmodium* bc_1 complex is the target of atovaquone that is used in combination with proguanil for the treatment and prevention of malaria (Siregar et al., 2015). NDH2 and SDH have been demonstrated to be essential for oocyst development in the mosquito stage and suggested as potential targets for developing transmission-blocking drugs (Boysen and Matuschewski, 2011; Hino et al., 2012; Ke et al., 2019). Licochalcone A, a natural chalcone isolated from the root of *Glycyrrhiza glabra* or *G. inflate,* was shown to inhibit SDH and bc_1 complex activities in isolated *P. falciparum* mitochondria (Mi-Ichi, 2005).

This study was conducted to identify the active antimalarial compound(s) contained in the ethanolic extract of leaf from *A. altilis* and gain insights into its mechanism of action. Here, we show that a geranylated dihydrochalcone purified from the ethanolic extracts of *A. altilis* leaves is the main anti-plasmodial compound and describe its effect on the food vacuole and the mitochondrial ETC of *P. falciparum.*

2. Material and methods

2.1. Plant material

The leaves of *A. altilis* were collected from Purwodadi Botanical Garden, East Java, Indonesia. A qualified botanist from this Garden conducted authentication and identification of this plant. A voucher specimen (No: B-107/IPH.06/AP.01/II/2020) of this raw material was stored at the Herbarium of the Institute of Tropical Disease, Universitas Airlangga, Surabaya, Indonesia.

2.2. Extraction, fractionation, and identification of active compound

Bioactivity-guided isolation was conducted to identify the active antimalarial compounds. One kilogram of dried leaves was macerated using 10 L of ethanol: water (8:2, *v/v*) for 4 h and then filtered. The process was repeated three times. The ethanolic extract was combined and dried using a rotary evaporator and weighed afterward. The dried extract was kept in an airtight container and stored at 4 °C until fractionation and antimalarial bioassay. An active fraction was further

fractionated under vacuum liquid chromatography (VLC) with a gradient of *n*-hexane and ethyl acetate (100%–0%). Based on thin-layer chromatography (TLC) profiles, several fractions were combined. The active fraction was then separated by semi-preparative High-Pressure Liquid Chromatography (HPLC, Shimadzu LC-06) method using methanol: water (8:2, *v/v*) at 1 mL/min of flow rate. The separation of the active fraction resulted in three isolates which were assayed for their antimalarial activity. The active isolate was analyzed using TLC and HPLC. TLC was performed using a silica gel 60 F_{254} plates, scanned by a TLC Visualizer on UV at 254 nm and 366 nm, and sprayed with H_2SO_4: water (1:9, *v/v*) to highlight the flavonoid compounds. The HPLC system included two LC-10AD pumps and an SCL-10A controller with an Agilent RP-18 XDB column (4.6 × 250 mm). The active isolate was eluted with methanol: water (8:2, *v/v*) at a 0.7 mL/min of flow rate. The chemical structure of the active isolate was determined using NMR-JEOL ECS 400 with $CdCl_3$ as the solvent, based on proton signals in the ^{1}H-NMR spectrum, carbon signals in the ^{13}C-NMR spectrum, heteronuclear multiple bond correlation (HMBC), heteronuclear multiple quantum correlation (HMQC), and correlation spectroscopy (COSY). The spectra were then analyzed using the MNova program. Mass spectra were identified by Agilent LC-MS-MS using methanol: water (8:2, *v/v*).

2.3. Parasite culture

P. falciparum strain 3D7 (chloroquine-sensitive strain) was obtained from the Malaria Laboratory, Centre of Natural Product Medicine Research and Development, Institute of Tropical Disease, Universitas Airlangga, Surabaya, Indonesia. The culture was established using the method described by Trager and Jensen with some modifications (Trager and Jensen, 1976). Parasites were grown in fresh human-type O-positive red blood cells (RBCs) at 5% haematocrit in complete RPMI-1640 medium (Sigma) supplemented with 10% (*v/v*) human type O-positive serum, 25 mM HEPES buffer (Applichem panreac), 50 μg/mL hypoxanthine (Sigma), 2 mg/mL $NaHCO_3$, and 10 μg/mL gentamycin (Sigma). The culture was incubated at 37 °C in a modified candle jar. Human RBCs and serum were received from The Indonesian Red Cross, Surabaya, Indonesia. The medium was replaced daily, and parasitemia was maintained below 5% for routine subculture. Parasitemia was determined by examining Giemsa's stained thin blood smears of infected RBCs (iRBCs). Parasite cultures were synchronized with 5% (*w/v*) D-sorbitol, as previously described (Lambros and Vanderberg, 1979).

2.4. In vitro antimalarial assay

Ten milligrams of the sample were diluted in 1 mL of dimethyl sulfoxide (DMSO). The sample was then further diluted in RPMI-1640 medium and used to prepare serial dilutions at final concentrations of 0.01, 0.1, 1, 10, and 100 μg/mL in a 24-well plate. A 500 μ L parasite culture (±1% parasitemia, 5% hematocrit) was added to each well and incubated for 48 h at 37 °C. After incubation, thin blood smears were stained using 10% (*v/v*) Giemsa dye. The percentage of parasitemia was determined by counting infected erythrocytes per 1000 total erythrocytes. The percentage of growth inhibition was calculated using the following equation:

$$100\% - \left(\frac{\mathrm{Xe}}{\mathrm{Xk}} \mathrm{x} 100\%\right)$$

where Xe is the average parasitemia of the experimental group and Xk is the average parasitemia of the negative control.

The IC50 values were calculated by applying a four-parameters logistic regression curve to the normalized dose-response data using GraphPad Prism 6.0 software (GraphPad Co. Ltd., San Diego, CA, USA). In line with WHO guidelines and basic criteria for antiparasitic drug discovery (Fidock et al., 2004; Pink et al., 2005), the activities of extracts were classified into four classes according to their IC_{50} values: high activity ($IC_{50} \leq 5$ μg/mL); promising activity (5 μg/mL< $IC_{50} \leq 15$ μg/mL); moderate activity (15 μg/mL < $IC_{50} \leq 50$ μg/mL); and weak activity ($IC_{50} > 50$ μg/mL). Meanwhile, isolated compound(s) were classified as highly active if the IC_{50} value was ≤1 μg/mL.

2.5. In vitro cytotoxicity assay on mammalian cell

DLD-1 cells were seeded at 2.5 × 10^4 cells/well on a 96-well plate and cultured overnight. The cells were then washed with PBS and replaced with a fresh medium. Test compounds or DMSO as control were then added to each well. After a 48-h incubation at 37 °C, the cells were then washed with PBS, 100 μL of a fresh medium, and 10 μL of Cell Counting Kit-8 (Dojindo) solution was added to each well. After a 3-h incubation, the absorbance was measured at 450 nm using a SpectraMax M2e-TUY microplate reader (Molecular Devices). According to the manufacturer's protocol, the cell viability of test wells was calculated based on the absorbance of control wells containing DMSO. Cytotoxicity (CC_{50}) against DLD-1 cell was calculated using nonlinear regression analysis by GraphPad Prism 6.0 software by applying the "log (inhibitor) vs. response–Variable slope (four parameters)" in "Dose-response–inhibition" equation family from a nonlinear regression analysis.

2.6. Impairment of P. falciparum stage development

Intraerythrocytic stage development inhibition assay was carried out against the synchronized *P. falciparum* 3D7 strain (using 5% (*w/v*) *D*-sorbitol) at a parasitemia of 0.3%, using 24-well culture plates and incubated at various time variations (0, 24, and 48 h). All experiment was performed in duplicate (each sample concentration was carried out twice on the same plate). A thin smear was made, stained with Giemsa, and the growth and development of the *Plasmodium* were observed using a light microscope (Olympus CH-20) with a 1000× magnification. The concentration used in this assay is the IC_{50} value of each material obtained from the previous antimalarial assay for the positive control (Chloroquine diphosphate), AAL-E, AAL-E.4, and (**1**) were 0.004 μg/mL, 0.48 μg/mL, 0.01 μg/mL, and 0.07 μg/mL, respectively.

2.7. Ultrastructural changes in food vacuoles revealed by transmission electron microscopy

Samples for TEM were carried out against the synchronized *P. falciparum* 3D7 strain (using 5% (*w/v*) *D*-sorbitol) at a parasitemia of 1%, using 24-well culture plates and incubated 24 h. Furthermore, samples were prepared using rOTO (reduced osmium thiocarbohydrazide osmium) and *en bloc* staining as described previously. *P. falciparum*-iRBCs were collected and fixed with 2% (*w/v*) glutaraldehyde in 0.1 M sodium cacodylate buffer pH 7.4 containing 1 mM $CaCl_2$ and 1 mM $MgCl_2$ for 1 h at 4 °C. The iRBCs were then rinsed with the cacodylate buffer and then post-fixed for 1 h at 4 °C with 1% (*w/v*) osmium tetroxide and 1.5% (*w/v*) potassium ferrocyanide in the cacodylate buffer. The cells were then washed with distilled water and incubated in 1% (*w/v*) thiocarbohydrazide solution for 20 min at room temperature. They were then washed with distilled water and fixed again with 1% (*w/v*) osmium tetroxide in distilled water for 30 min at room temperature. After washes with distilled water, the samples were stained *en bloc* with 1% (*w/v*) uranyl acetate in 75% ethanol overnight at 4 °C. After washing again with distilled water, they were stained with lead citrate for 30 min at 4 °C (Reynolds, 1963). After another distilled water rinse, the cells were dehydrated through a series of ethanol and acetone of ascending concentration and embedded in Quetol 651 epoxy resin (Nisshin EM). Thin sections were obtained using an ultramicrotome (Reichert-Jung) and observed by TEM (JEM-1230; JEOL).

2.8. Antimalarial activity against recombinant PfMQO

A Recombinant *Pf*MQO activity inhibition assay was conducted essentially as previously described (Hartuti et al., 2018; Ruan et al., 2019). Initially, extracts, fractions, and isolated compounds from *A. altilis* extract were tested against recombinant *Pf*MQO at a final concentration 100 μg/mL, respectively. The assay was briefly performed in an assay mix composed of 50 mM HEPES-KOH pH 7.0, 1 mM KCN, 25 μM decylubiquinone (dUQ), 120 μM DCIP, and 3 μg/mL of *Pf*MQO--membrane fraction. One microliter of tested samples was transferred to a 96-well plate, followed by 194 μL of assay mix. As a negative control (0% inhibition), 1 μL DMSO was applied to column 1. The background was recorded for 5 min at 600 nm and 37 °C using SpectraMax® Paradigm® Multi-Mode Microplate Reader (Molecular Devices). The reaction was started by ADDINg 5 μL of 400 mM malate into columns 1–11, and the activity was recorded for 10 min. Water (5 μL) was added in column 12 and was set as a positive control (100% inhibition). The *Pf*MQO inhibition was analyzed by calculating the inhibition (%) compared to negative control in triplicates. Hits were defined as extracts, fractions, and isolated compounds exhibiting >50% inhibition. Z′-factor, S/N, S/B, and SW were calculated as previously reported. The IC_{50} was determined by measuring the *Pf*MQO activity under serial dilutions of 100, 30, 10, 1, 3, 0.1, 0.3, 0.01, and 0.03, μg/mL for the extracts and fractions, and 100, 30, 10, 1, 3, 0.1, 0.3, 0.01, 0.03, and 0.001 μM for the isolated compound. The IC**50** values were calculated by applying a four parameters equation from nonlinear regression analysis to the normalized dose-response data using GraphPad Prism 6.0 software (GraphPad Co. Ltd., San Diego, CA, USA).

2.9. PfMQO inhibition mechanism with (1)

The inhibition mechanism of *Pf*MQO by (**1**) was evaluated by following the direct rate of dUQ consumption at 37 °C and 278 nm in 1 cm black quartz cuvette. The assay buffer contained HEPES-KOH pH 7.0, 1 mM KCN, 1.25 μg/mL PfMQO membrane. Determination of *Pf*MQO inhibition for dUQ binding site was performed by measuring *Pf*MQO activity at 2, 4, 6, 8, 10, 12, 14, 16, 18, 20, 22, and 24 μM of dUQ (final concentration) at fixed malate concentration of 10 mM, whereas the concentration of compound applied were 0, 0.5, 1, and 2 μM. Moreover, the determination of *Pf*MQO inhibition for the malate binding site was assayed at 0.5, 1, 2, 4, 6, 8, 10, 12, 14, 16, 18, and 20 mM malate at fixed dUQ concentrations of 20 μM and concentration of compound at 0, 0.5, 1, and 4 μM.

2.10. Counter assay activity of (1) to mammalian electron transport chain enzymes

The (**1**) was assayed against NADH-cytochrome *c* (complex I-III activities) and succinate-cytochrome *c* (complex II-III activities) using bovine heart mitochondria prepared as previously reported (Miyazaki et al., 2018). The (**1**) was prepared in serial dilutions at concentrations of 100, 30, 10, 3, 1, 0.3, 0.1, 0.03, 0.01, and 0.003 μM. The assay was performed by measuring the reduction of cytochrome *c* at 550 nm in quadruplicates using 96-well plates. In the NADH-cytochrome *c* assay, the reaction buffer contained 50 mM phosphate buffer pH 7.4, 2 mM KCN, 200 μM cytochrome *c*, and 15 μg/mL bovine heart mitochondria, which was started by the addition of 0.3 mM NADH. A similar measurement was conducted for succinate-cytochrome *c* inhibition with a small modification in cytochrome *c* (100 μM) and bovine heart mitochondria concentrations (25 μg/mL). The reaction was started by the addition of 10 mM succinate as a substrate into the wells. DMSO was added into the first column as the negative control (0% inhibition), with 5 μM ascochlorin in column 12 as the positive control (100% inhibition). As references, ferulenol (*Pf*MQO inhibitor), brequinar (human DHODH inhibitor), asochlorin (complex III inhibitors), and rotenone (complex I inhibitor) which are classical ETC inhibitors, were also assayed (Miyazaki et al., 2018).

2.11. Transgenic parasite expressing cytosolic yeast dihydroorotate dehydrogenase (yDHODH)

Parasites expressing yDHODH-GFP were obtained by transfection of pHHyDHODH-GFP plasmid (Kerafast, Boston, MA, USA) to 3D7 parasites following an established method (Deitsch, 2001). Briefly, 50 μg of plasmid dissolved in cytomix solution (120 mM KCl, 0.15 mM $CaCl_2$, 10 mM K_2HPO_4/KH_2PO_4 pH 7.6, 25 mM HEPES, 2 mM EGTA, and 5 mM $MgCl_2$) into RBCs using Gene Pulser Xcell (Bio-rad). Percoll-sorbitol synchronized parasites were mixed with these RBCs containing the plasmid and maintained under 5 nM WR99210 for 2 weeks. Once the transfectant parasites were obtained, the expression of yDHODH was confirmed by assaying the parasite resistance to DSM265 (*Pf*DHODH inhibitor) and atovaquone (Complex III inhibitor) by *Pf*LDH/diaphorase assay as previously described (Hartuti et al., 2018). All experiment was performed in quadruplicate measurements on the same plate.

2.12. Isobologram analysis of (1) with atovaquone and chloroquine

The antimalarial activity of (**1**) and in combination with atovaquone and chloroquine was investigated by *Pf*LDH/diaphorase assay as previously described (Hartuti et al., 2018; Wang et al., 2019). In each combination assay between two compounds: atovaquone and (**1**), chloroquine and (**1**), atovaquone and chloroquine, were combined in four fixed ratios of concentration (4:1, 3:2, 2:3, and 1:4). Two fixed ratios concentration (5:0 and 0:5) used for determined the IC_{50} of each drug alone. Serial dilutions of each combination were prepared, and 100 μL was transferred into 96-well culture plates. Next, 100 μL cultures of 0.3% synchronized ring form parasites were transferred into each plate containing the dilutions. The plates were arranged in a clean, modular incubation chamber, flushed with mixed gas (gas has 90% N_2, 5% CO_2, 5% O_2) for 10 min, and incubated for 72 h at 37 °C. After incubation, parasite growth was monitored by the *Pf*LDH/diaphorase assay using a SpectraMax® Paradigm® Multi-Mode Microplate Reader (Molecular Devices). The IC_{50} values were calculated using GraphPad Prism®ver.6.0 software. The effect of drug combination was evaluated by using isobolographic analysis as previously described (Agarwal et al., 2015; Fivelman et al., 2004). The IC_{50} was calculated from parasite culture in (**1**) and combination culture with atovaquone and chloroquine for each combination. The following equation determined the FIC value:

$$FIC = \frac{IC_{50} \text{ of compound A mixture}}{IC_{50} \text{ of compound A}}$$

The following equation determined the combination index (CI):

$$CI = \frac{IC_{50} \text{ of compound A in mixture}}{IC_{50} \text{ of compound A}} + \frac{IC_{50} \text{ of compound B in mixture}}{IC_{50} \text{ of compound B}}$$

$CI < 1$ represents synergism, $CI = 1$ represents additive effect, $CI > 1$ represents antagonism.

3. Results

3.1. Extraction, fractionation, and identification of active compound

Dried powder of *A. altilis* leaves extracted using 80% ethanol at 40 °C by maceration methods. The crude extract (AAL-E) was then further fractionated by the VLC method using a gradient solvent of n-hexane and ethyl acetate (100%–0%), resulting in 6 fractions (AAL-E.1 - AAL-E.6). All fractions were inhibited *P. falciparum* growth. Fraction AAL-E.4 showed the most potent inhibition with an IC_{50} of 0.01 μg/mL and was selected for further purification of the active compound by semi-preparative HPLC. We obtained three isolates (AAL-E.4.1, AAL-E.4.2,

and AAL-E.4.3) from fraction AAL-E.4. Amongst the isolates, only AAL-E.4.2 (**1**) showed inhibition against *P. falciparum*, while two other isolates were inactive.

The structure of (**1**) was then determined based on proton and carbon signals in the ^{1}H and ^{13}C-NMR spectrum, HMBC, HMQC, and COSY. The ^{13}C-NMR spectrum of (**1**) showed 25 signals for 25 carbon atoms, consisting of one conjugated carbonyl carbon (δC 203.9 ppm). The UV spectrum of (**1**) at a concentration of 0.5 mg/mL showed the maximum absorption at λ_{max} 206, 248, 278, and 314 nm, corresponding to a substituted benzoyl chromophore (Syah et al., 2006). The ^{1}H NMR spectrum showed the presence of 2 aromatic rings, ring A and ring B. Ring A structure can be confirmed from the aromatic protons, which showed ABX system at δH 6.37 (1 H, d, J = 2.4 Hz, H-3′), δH 6.35 (1 H, J = 8.4 Hz, H-5′), and δH 7.59 (1H, d, J = 8.4 Hz, H-6′). The (**1**) contained one geranyl group (signals at δH 5.17 (brt, J = 6, H-2”), 5.03 (brt, J = 5.6, H-6”), 3.40 (d, J = 6.8, H-1″), 2.09 (q, J = 6.4, H-5″), 2.058 (H-4″), 1.78 (brs, H-8″), 1.67 (brs, H-10″), 1.571 (brs, H-9″) ppm). Two triplet signals of the methylene group at δH 3.11 (t, J = 6.8, H- α) and 2.97 (t, H – β) ppm for methylene-α and -β were observed. Furthermore, the signal at the aromatic ring showed there was a 1,2,3,4- tetrasubstituted benzene unit (δH 6.70 (d, J = 8, H-5) and 6.67 (d, J = 8.4, H- 6) (ppm) and a 2,4-dihydroxy benzoyl group (δH 7.59 (d, J = 8.4, H-6′), 6.36 (d, J = 2.4, H-3′), and 6.35 (dd, J = 8.4, 2.4, H-5′ ppm). Comparing the NMR spectrum with the references, we concluded that (**1**) is 2-geranyl-2′, 4′, 3, 4-tetrahydroxy-dihydrochalcone (Fig. 1).

The molecular structure of (**1**) was confirmed by the Agilent LC system coupled with Q-TOF/MS for HRESIMS analysis. HR-MS measurement revealed an ion peak $[M+H]^{+}$ at m/z 409.2039 (calculated 410.55) consistent with the molecular formula of $C_{25}H_{30}O_5$.

3.2. In vitro antimalarial and mammalian cytotoxicity

The result of the antimalarial assay showed dose-dependent *P. falciparum* growth inhibition of AAL-E, all fractions (AAL-E.1 - AAL-E.6), and (**1**) (Table 1). The IC_{50} values of all assayed samples ranged from 0.01 to 3.52 μg/mL and are within the criteria mentioned by WHO guidelines and basic criteria for antiparasitic drug discovery as antimalarial with high activity. Amongst the fractions tested, AAL-E.4 showed the best antimalarial activity with an IC_{50} value of 0.01 μg/mL. Purification of AAL-E.4 resulted in three isolates (AAL-E.4.1 - AAL-E.4.3). Isolate AAL-E.4.1 and AAL-E.4.3 did not exhibit antimalarial activity. On the other hand, AAL-E.4.2 (**1**) showed highly active antimalarial activity with an IC_{50} value of 0.07 μg/mL (0.17 μM). According to the cytotoxicity test, (**1**) was moderately toxic to DLD-1 cells with a CC_{50} value of 19.7 ± 2.18 μM and a selectivity index of 115.8.

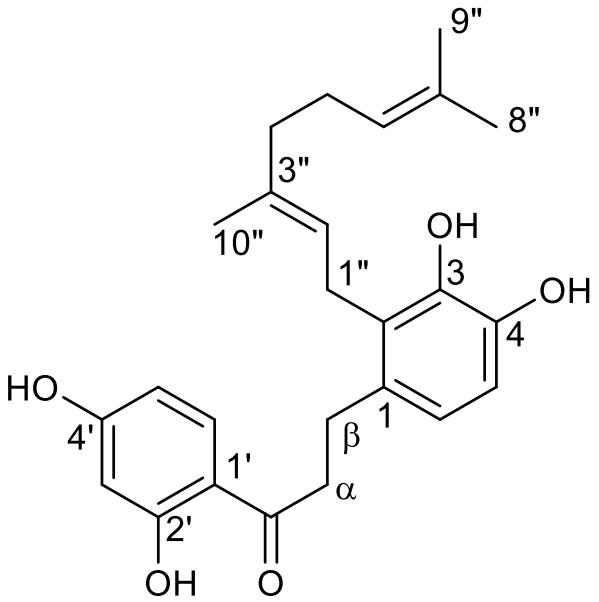

Fig. 1. Chemical structure of (**1**).

Table 1
The IC_{50} value of all samples against *Plasmodium falciparum* 3D7. Growth inhibition was evaluated by the microscopic assay as described in the material and methods section.

Sample	IC_{50} (μg/mL)
AAL-E	0.48 ± 0.04
AAL-E.1	2.31 ± 0.41
AAL-E.2	3.52 ± 1.32
AAL-E.3	1.32 ± 0.11
AAL-E.4	0.01 ± 0.01
AAL-E.5	0.71 ± 1.46
AAL-E.6	1.76 ± 0.26
AAL-E.4.1	Inactive
AAL-E.4.2 (**1**)	0.07 ± 0.03
AAL-E.4.3	Inactive
Chloroquine	0.04 ± 0.00

Data are presented as the average of double measurements.

3.3. Impairment of P. falciparum stage development effect on food vacuole

The (**1**) impaired the *P. falciparum* staged development compared to negative controls, as shown in Fig. 2. After synchronization of the parasite, ring stages were observed at the start of incubation (0 h) in all conditions, as expected. Impairment of *P. falciparum* stage development could be observed after 24 h of incubation for the positive control (chloroquine), AAL-E.4, and (**1**) groups, where the ring stage was still dominant. In contrast, the negative control (DMSO) and AAL-E showed development to the schizont stage. After 48 h of incubation, there were no schizont-stage parasites in the positive and negative control groups. In the AAL-E, AAL-E.4, and (**1**) groups, parasites were predominantly in the schizont stage. Therefore, we concluded that AAL-E, AAL-E.4, and (**1**) inhibit the *Plasmodium*'s stage development, causing an accumulation of the schizont stage after 48 h of incubation.

Electron microscopy was carried out to examine the changes in the ultrastructure of food vacuole in *P. falciparum*-iRBCs exposed to AAL-E, AAL-E.4, and (**1**). As shown in Fig. 3, several inner vesicles were observed in the food vacuoles of *P. falciparum* exposed to AAL-E (Fig. 4A), AAL-E.4 (Fig. 4B), and (**1**) (Fig. 4C) but not in DMSO (Fig. 4D).

3.4. Antimalarial activity against recombinant PfMQO

To determine the effect of (**1**) against *Pf*MQO, we tested the crude extract and the fractions obtained during the purification and the isolated compounds. As a result, the AAL-E, four fractions (AAL-E.3, AAL-E.4, AAL-E.5, and AAL-E.6), and (**1**) inhibited r*Pf*MQO at an IC_{50} less than 10 μg/mL or 10 μM for the extracts and (**1**), respectively. As the positive control, ferulenol, previously reported to inhibit r*Pf*MQO, showed an IC_{50} of 0.17 μM (Table 2). The quality control of the assay was monitored by calculating several parameters, including Z′-factor, S/B, S/N, and CV (%) with values of 0.84, 7.42, 266.4, and 4.31, respectively, indicating the high quality and performance of the assay. Moreover, the mechanism of inhibition of (**1**) was investigated, and as shown in Fig. 4, the parallel lines of the double reciprocal plot under varying malate concentrations indicate that (**1**) is an uncompetitive inhibitor *versus* malate. On the other hand, when the concentration of dUQ was varied, the plot yielded lines intersecting at X-axis, indicating that (**1**) is a non-competitive inhibitor *versus* dUQ. This result indicates that (**1**) binds specifically to the *Pf*MQO-malate complex and that the ternary

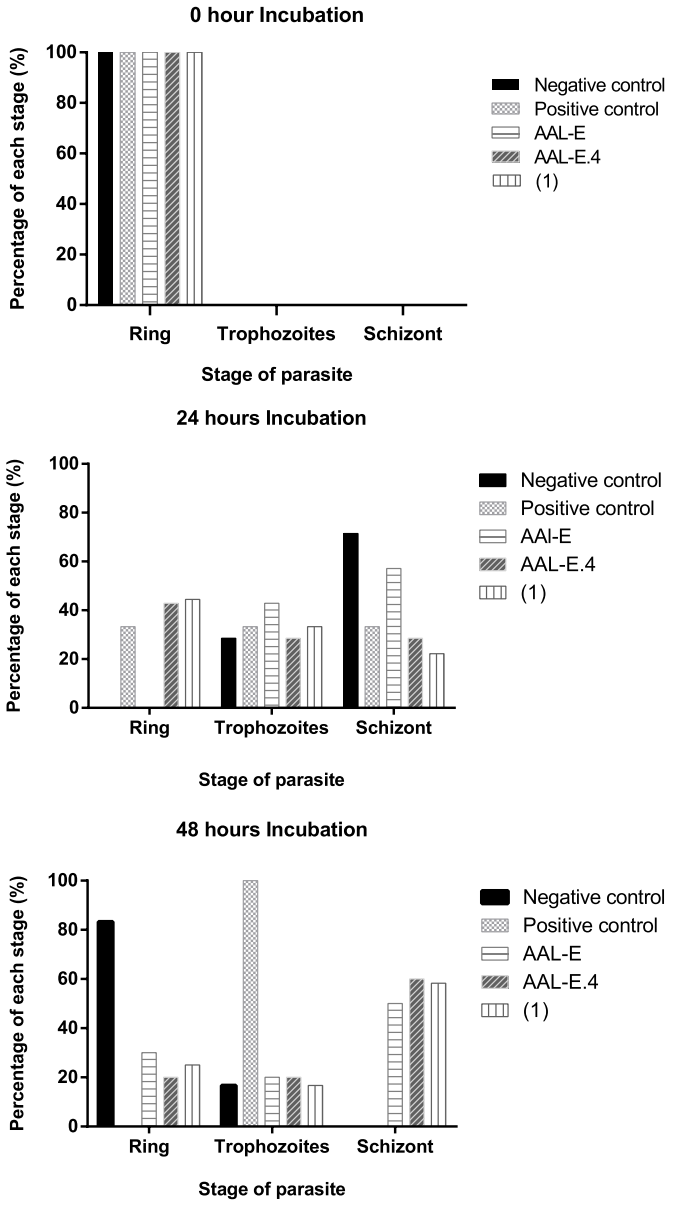

Fig. 2. Histogram of stage development percentage of *Plasmodium falciparum* treated with negative control, positive control, AAL-E, AAL-E.4, and (**1**) for 0, 24, and 28 h of incubation. Data are presented as the average of duplicate measurements (each sample concentration was carried out twice on the same plate).

complex (*Pf*MQO-malate-(**1**)) does not react with dUQ. This supports the notion that in addition to malate and ubiquinone binding sites, the *Pf*MQO has a third binding site where (**1**) binds.

3.5. Counter assay activity of (1) to mammalian electron transport chain enzyme

The potential inhibition of (**1**) to mammalian respiratory complexes was evaluated using bovine heart mitochondria. Rotenone, ascochlorine, brequinar, and ferulenol were used along with (**1**) as controls. For NADH-cytochrome *c* (complex I-III) activity, inhibition was observed for rotenone, ascochlorine, and ferulenol with IC_{50} values of 0.01 ± 0.00, 0.01 ± 0.00, and 0.28 ± 0.08 μM, respectively. For succinate-cytochrome *c* (complex II-III) activity, rotenone, ascochlorine, brequinar, and ferulenol inhibited this reaction with IC_{50} values of 1.86 ± 0.11, 0.01 ± 0.00, 22.94 ± 1.46, and 0.17 ± 0.01 μM, respectively (Table 3). The IC_{50} values of (**1**) against complex I-III and complex II-III were 13.58 ± 2.19 and 10.83 ± 0.65 μM, respectively. These results showed that inhibition of the mammalian ETC enzyme starts at micromolar concentration.

3.6. Transgenic parasite expressing cytosolic yeast dihydroorotate dehydrogenase (yDHODH)

Previously, it has been described that *P. falciparum* 3D7 strain expressing yDHODH (yDHODH-3D7) becomes resistant to DHODH and bc_1 complex inhibitors (Painter et al., 2007). Accordingly, yDHODH-3D7 strain is a good model to verify whether or not a compound's target is one of these two enzymes. To further analyze the possibility of (**1**) inhibiting *P. falciparum* DHODH and bc_1 complex, the IC_{50} values of (**1**) against *P. falciparum* 3D7 and yDHODH-3D7 strains were determined as 10.4 and 11.6 μM, respectively (Fig. 5).

3.7. Isobologram analysis of (1) with atovaquone and chloroquine

The isobologram analysis was conducted to check a possible interaction of (**1**) with atovaquone, (**1**) with chloroquine, and atovaquone with chloroquine. The sum of FICs is represented in isobolograms (Fig. 6). The isobologram assay of **(1)** and atovaquone showed that all fixed-ratio combinations were antagonistic interactions. The combination (**1**) and chloroquine showed that 3 out of 4 combinations had antagonistic interactions, and only 1 showed synergism interaction. It was similar to the combination of chloroquine and atovaquone. These results indicated that the 3 combinations have antagonistic interactions.

4. Discussion

This study has isolated the main active constituent from *A. altilis* leaves, namely as 2-geranyl-2′, 4′, 3, 4-tetrahydroxy-dihydrochalcone (**1**), and show its antimalarial activity for the first time. We also demonstrate that (**1**) has potent antimalarial activity by inhibiting *P. falciparum's* growth with an IC_{50} value of 0.17 μM. Moreover, compound (**1**) showed low toxicity to DLD-1 cells with CC_{50} of 19.7 μM and a selectivity index of 115.8.

The presence of geranylated derivatives of dihydrochalcone from *A. altilis* leaves has been reported, including (**1**) in leaves of *A. altilis* from Thailand and Indonesia (Shimizu et al., 2000; Syah et al., 2006). The (**1**) has also been found in other subspecies, including *A. communis*, *A. incises*, and *A. nobilis* (Jayasinghe et al., 2004; Patil et al., 2002; Shimizu et al., 2000). Inhibition of several biological pathways has been suggested to be associated with the biological activity of (**1**) such as 5-lipoxygenase (Fujimoto et al., 1987), which plays a key role in allergic processes, and cathepsin K (Fujimoto et al., 1988), a cysteine protease involved in inflammation, and in the pathogenicity of osteoporosis (Koshihara et al., 1988). The potential of (**1**) as an antiallergic and antitumor agent has been patented (Fujimoto et al., 1987, 1988), as well as the method of its chemical synthesis (Nakano and Uchida, 1990).

We have been previously isolated from the leaves of *A. altilis* 1-(2,4-dihydroxy phenyl)-3-(8-hydroxy-2-methyl-2-(4-methyl-3-pentenyl)-2H-1-benzopyran-5-yl]-1-propanone, which is a dihydrochalcone derivative with a chemical structure similar to (**1**), with an IC_{50} of 1.05 μM against *P. falciparum* 3D7 strain, and suggested to inhibit the falcipain-2, a cysteine protease localized in parasite's food vacuole and involved in hemoglobin digestion (Hidayati et al., 2020). In this study, we showed that the antimalarial activity of **(1)** surpassed the previous isolate despite a similar chemical structure.

The mechanism of action of (**1**) was investigated by analyzing the *P. falciparum* 3D7 intraerythrocytic stage development. In the positive control group, chloroquine showed potent activity with the accumulation of trophozoite after 48 h incubation. Moreover, compared to the negative control (DMSO), parasites were enriched at the schizont stage by incubation with (**1**) after 48 h. This result indicates that (**1**) can

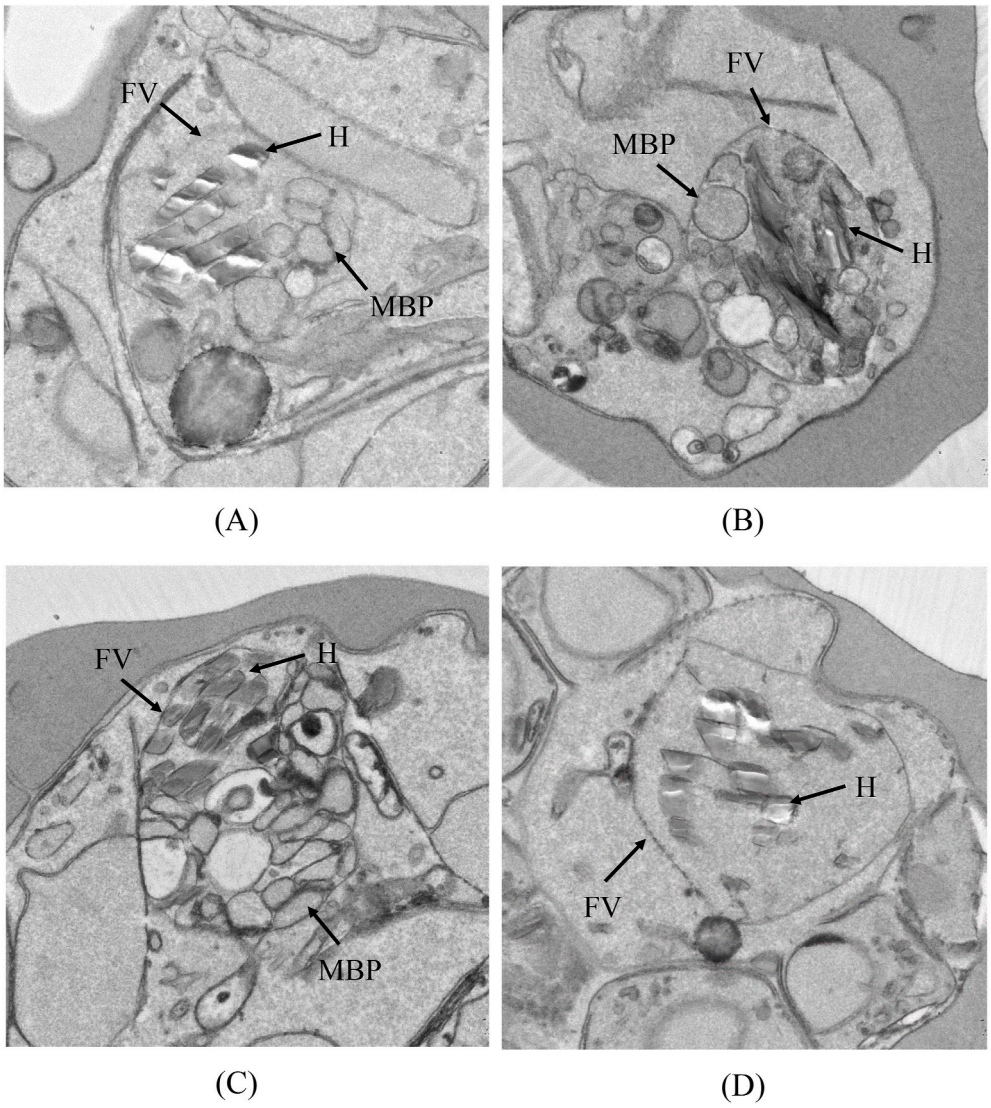

Fig. 3. Transmission electron micrographs of *Plasmodium falciparum* after 24 h incubation with AAL-E (A), AAL-E.4 (B), and (**1**) (C), and negative control (D). Figures A, B, and C show several inner vesicles in the food vacuole (FV) of *P. falciparum*. Scale bars are 500 nm.

clearly delay the parasite's stage development from the ring to the schizont stage. Interestingly, TEM analysis of the parasite incubated with the active fractions and (**1**) showed ultrastructural alterations characterized by the formation of several inner vesicles inside the food vacuole, which resemble undigested hemoglobin vesicles (Biagini et al., 2003; Hoppe et al., 2004) leading to growth inhibition or parasite death (Sachanonta et al., 2011; Yayon et al., 1984).

Licochalcone A, a natural chalcone isolated from *G. inflata* (Xinjiang licorice), has been previously demonstrated to inhibit *P. falciparum* ETC at the level of *bc*1 complex (Ke et al., 2019). It is largely accepted that an important function of the *P. falciparum bc*1 complex at the intra-erythrocytic stage is to regenerate ubiquinone to be used as the electron acceptor for *Pf*DHODH, which belongs to family 2 and catalyzes the rate-limiting step in the pyrimidine *de novo* biosynthesis (Birth et al., 2014). Some organisms, such as budding yeast and Trypanosomatids, possess the family 1A DHODH, a cytosolic enzyme that uses fumarate as the electron acceptor and is resistant to family 2 DHODH inhibitors targeting the ubiquinone binding site (Inaoka et al., 2008). Consistently, *P. falciparum* expressing yDHODH confer resistance to *bc*1 complex and DHODH inhibitors (Hartuti et al., 2018; Inaoka et al., 2016). To determine whether (**1**) inhibits these two enzymes, growth inhibition of (**1**) in *P. falciparum* 3D7 (WT) and 3D7-*y*DHODH strains were investigated, and according to the IC_{50}s of 10.4 μM and 11.6 μM, respectively, we show that (**1**) does not inhibit parasite's *bc*1 complex either DHODH.

Among the ETC enzymes, MQO was recently unable to knockout in *P. falciparum* (Wang et al., 2019). In *P. berghei*, MQO knockout parasites are viable, at least in the intraerythrocytic stage. However, those mutants showed impaired growth, were unable to induce cerebral malaria in an animal model, and have been suggested to be essential for virulence (Niikura et al., 2017). Recently, recombinant *Pf*MQO has been characterized, and its first inhibitor (ferulenol) was found to inhibit *P. falciparum* growth and displayed a synergic effect in combination with atovaquone (Hartuti et al., 2018). This phenotype was attributed to the trifunctionality of *Pf*MQO where it plays an important role in ETC, TCA cycle, and fumarate cycle (Bulusu et al., 2011; Jayaraman et al., 2012; Ke et al., 2015). To test the potential inhibition of *Pf*MQO activity, recombinant *Pf*MQO overexpressed in the bacterial membrane was used, and it found that (**1**) inhibited *Pf*MQO activity in a dose-dependent manner with an IC_{50} of 2.15 ± 0.29 μM. It has been previously suggested that the ferulenol binding site is distinct from the ubiquinone binding site, suggesting a third binding site for inhibitors (Hartuti et al., 2018; Yamashita et al., 2018).

Finally, the possibility of (**1**) inhibition on the mammalian ETC enzymes was investigated, and (**1**) showed similar inhibition profiles to

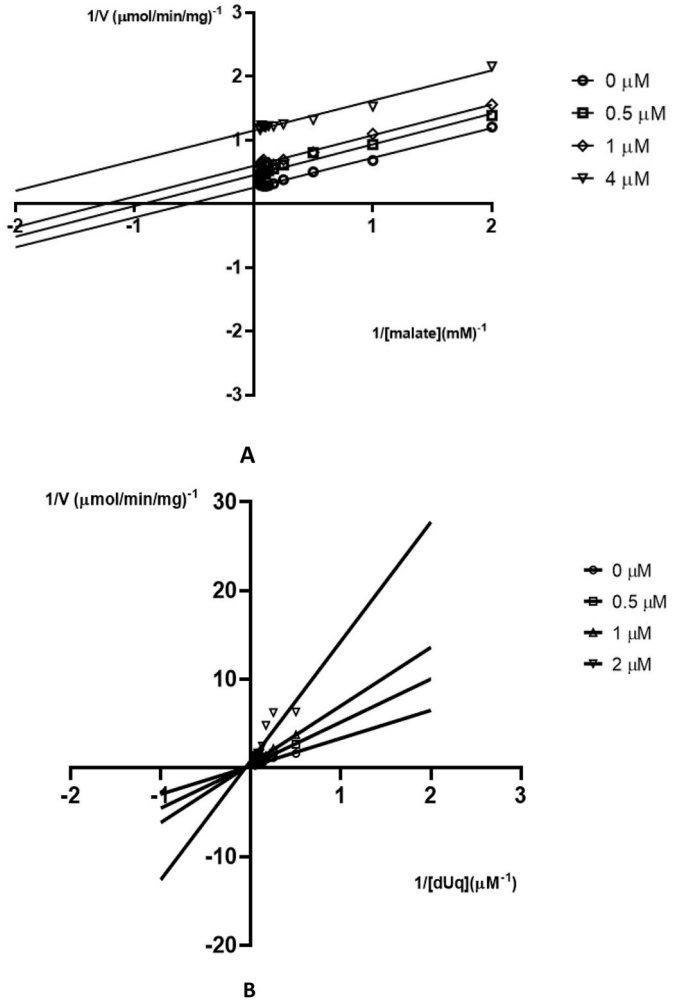

Fig. 4. Inhibition mechanism of **(1)** against recombinant *Pf*MQO. The (1) is an uncompetitive and noncompetitive inhibitor versus malate (A) and dUQ (B) of *Pf*MQO, respectively.

Table 2
The IC_{50} value of all samples against recombinant *Pf*MQO.

Sample	IC_{50} (μg/mL)
AAL-E	9.53 ± 1.03
AAL-E.1	Inactive
AAL-E.2	Inactive
AAL-E.3	4.39 ± 0.32
AAL-E.4	1.97 ± 0.20
AAL-E.5	3.49 ± 0.25
AAL-E.6	4.68 ± 0.14
AAL-E.4.1	Inactive
AAL-E.4.2 (**1**)	2.15 ± 0.29
AAL-E.4.3	Inactive
Ferulenol	0.06 ± 0.01

Data are presented as the average of triplicate measurements.

complex I-III and II-III activities. Considering that complex I and II inhibitors do not share cross-sensitivity, we can conclude that (**1**) can inhibit mammalian complex III at high (micromolar order) concentrations.

Table 3
Effect of (**1**) against succinate-cytochrome *c* (complex I-III) and (complex II-III) compared with the effect of aschoclorine, brequinar, ferulenol, and rotenone as ETC inhibitors.

Sample	IC_{50} of the sample against succinate-cytochrome *c* (complex I-III) (μM)	IC_{50} of the sample against succinate-cytochrome *c* (complex II-III) (μM)
(**1**)	13.58 ± 2.19	10.83 ± 0.65
Ascochlorin	0.01 ± 0.00	0.01 ± 0.00
Brequinar	30.00 ± 0.00	22.94 ± 1.46
Ferulenol	0.28 ± 0.08	0.17 ± 0.01
Rotenone	0.01 ± 0.00	1.86 ± 0.11

Data are presented as the average of triplicate measurements.

5. Conclusion

In this study, we showed the isolation of (**1**) from the leaves of *A. altilis* as the antimalarial constituent. Moreover, we demonstrated that (**1**) affects the ultrastructure of parasite's food vacuole, impairing the hemoglobin digestion and also inhibits *Pf*MQO. Because *P. falciparum* depends on active ETC and TCA cycle for the development in all life cycle stages, the ability of (**1**) to inhibit *Pf*MQO offers a great advantage over chloroquine, which acts exclusively at the intra-erythrocytic stage. Such a dual-organellar mechanism of action of (**1**) can be explored to develop novel antimalarial drugs active against multiple life cycle stages and reduce the risk of selecting resistant parasites. Further research is needed to decrease the toxicity value (**1**) by performing molecule structure modification of (**1**) to obtain compounds that have the same antimalarial activity but are not toxic to mammalian mitochondria.

Author Contributions

Author Contributions: Conceptualization, K.K, D.K.I., T.N, A.F.H., D. S., and A.W.; Methodology, D.K.I, E.Y., F.T., T.S., M.S., J.O., A.F.H., D.S., and A.W.; Isolation and Structure Elucidation A.R.H., M., L.T., M.T, A. W., A.F.H., K.D., and M.M.; *P. falciparum in vitro* culture and antimalaria assay H.I., T.S., A.R.H. and D.W; cytotoxicity assays on mammalian cell J.O and H.I.; stage development observation A.R.H., H.I., D.S. and A.W.; ultrastructural changes in food vacuoles observation M.S., A.R,H. and D. S., antimalarial activity against recombinant *Pf*MQO, Counter assay of (**1**) activity to mammalian ETC enzyme D.K.I., E.D.H., H.I., and A.R.H.; *in vitro* antimalarial drugs interaction assay T.S., H.I. and A.R.H; yDHODH-3D7 parasite and transgenic strain assay E.T., F.T. and T.S.; Data analysis, D.K.I., M.M., T.S., M.T., A.F.H., D.S., and A.W; Investigation, A.R.H., H.I., T.S., M.S., J.O., E.D.H., and D.K.I.; Resources, K.K., E.Y., F.T., D.K.I, T.S., A.F.H. and A.W.,: Writing-Original Draft Preparation, A.R.H., H.I, E.D.H., T.S., M.S., D.K.I., and A.W.; Visualization, H. I. and D.K.L; Supervision, T.S., D.K.L, D.S., A.F.H, and A.W.; Funding Acquisition, K.K, T.N, D.K.I., A.F.H., and A.W.

Funding

This work was funded in part by the Directorate General of Higher Education grant from World-Class Research 2020) (no.945/UN3.14/LT/2020 to A.F.H. and A.W.), and in part by Infectious Disease Control from the Science and Technology Research Partnership for Sustainable Development (SATREPS, nos. 10000284 to K.K. and 14425718 to T.N. and D.K.I.) from AMED/JICA and Grants-in-aid for Scientific Research (C) (no. 19K07523 to D.K.I.); and in part by Grants-in-aid for Research on Emerging and Re-emerging Infectious Diseases from the Japanese Ministry of Health and Welfare (no. 17929833 to K.K. and T.N. and no. 20314363 to D.K.I. and T.N.).

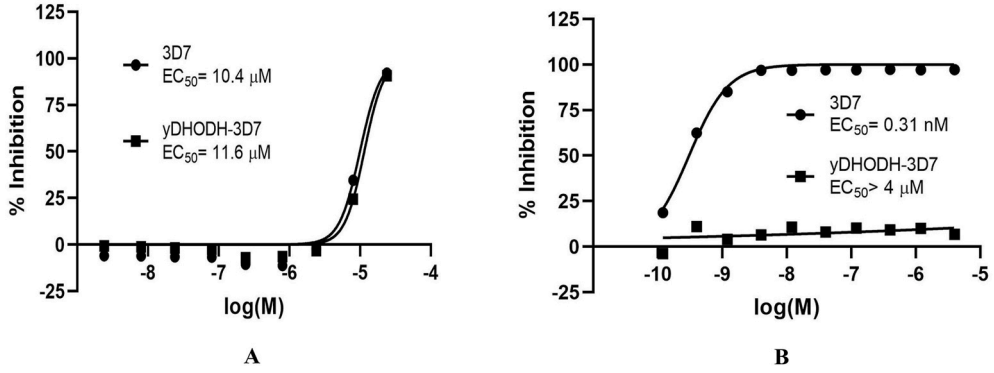

Fig. 5. Inhibition of (**1**) (A) and atovaquone (B) against wild type *P. falciparum* 3D7 and yDHODH-3D7. Data are presented as the average of quadruplicate measurements on the same plate.

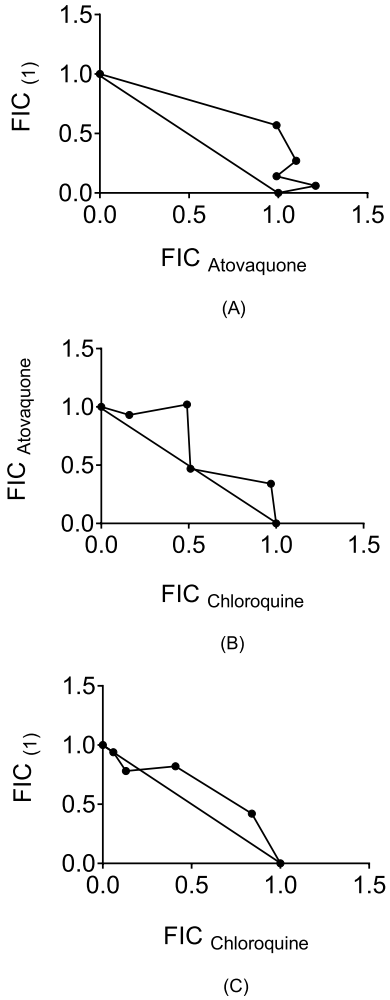

Fig. 6. Isobolograms analysis of (**1**) versus atovaquone (A), chloroquine and atovaquone (B), and (**1**) and chloroquine (C) against *Plasmodium falciparum* 3D7. The line-of-additivity is shown connecting the FIC = 1.0 from both compounds. The drug-combination curve below this line (FIC <1.0) indicates synergism, while above (FIC >1.0) indicates antagonism. All concentrations of (**1**) and atovaquone (A) showed antagonism. The concentration of (**1**) and chloroquine (C) and chloroquine and atovaquone (B) also showed antagonism, but there was a concentration that showed synergism.

Declaration of competing interest

The authors declare that there are no conflicts of interest in this study.

Acknowledgments

The author is grateful to all the staff from the Department of Molecular Infection Dynamics and Central Laboratory, Institute of Tropical Medicine (NEKKEN), and School of Tropical Medicine and Global Health at Nagasaki University for providing facilities and help in the enzymatic assay and transmission electron microscopy. The authors thank the Japanese Red Cross Society for providing human RBC (registry no. 30J0046).

References

Agarwal, D., Sharma, M., Dixit, S.K., Dutta, R.K., Singh, A.K., Gupta, R.D., Awasthi, S.K., 2015. In vitro synergistic effect of fluoroquinolone analogues in combination with artemisinin against Plasmodium falciparum; their antiplasmodial action in rodent malaria model. Malar. J. 14, 48. https://doi.org/10.1186/s12936-015-0561-2.

Akanbi, T., Saari, N., Adebowale, A.-R., 2009. Functional and pasting properties of a tropical breadfruit (Artocarpus altilis) starch from Ile-Ife, Osun state, Nigeria. Int. Food Res. J. 16, 151–157.

Balbach, A., 1992. As Frutas Na Medicina Natural. A Verdade Presente.

Biagini, G.A., Bray, P.G., Spiller, D.G., White, M.R.H., Ward, S.A., 2003. The digestive food vacuole of the malaria parasite is a dynamic intracellular Ca2+ store. J. Biol. Chem. 278, 27910–27915. https://doi.org/10.1074/jbc.M304193200.

Birth, D., Kao, W.-C., Hunte, C., 2014. Structural analysis of atovaquone-inhibited cytochrome bc1 complex reveals the molecular basis of antimalarial drug action. Nat. Commun. 5, 4029. https://doi.org/10.1038/ncomms5029.

Boysen, K.E., Matuschewski, K., 2011. Arrested oocyst maturation in Plasmodium parasites lacking type II NADH:Ubiquinone dehydrogenase. J. Biol. Chem. 286, 32661–32671. https://doi.org/10.1074/jbc.M111.269399.

Bulusu, V., Jayaraman, V., Balaram, H., 2011. Metabolic fate of fumarate, a side product of the purine salvage pathway in the intraerythrocytic stages of Plasmodium falciparum. J. Biol. Chem. 286, 9236–9245. https://doi.org/10.1074/jbc.M110.173328.

Cui, L., Mharakurwa, S., Ndiaye, D., Rathod, P.K., Rosenthal, P.J., 2015. Antimalarial drug resistance: literature review and activities and findings of the ICEMR network. Am. J. Trop. Med. Hyg. 93, 57–68. https://doi.org/10.4269/ajtmh.15-0007.

Deitsch, K.W., 2001. Transformation of malaria parasites by the spontaneous uptake and expression of DNA from human erythrocytes. Nucleic Acids Res. 29, 850–853. https://doi.org/10.1093/nar/29.3.850.

Fidock, D.A., Rosenthal, P.J., Croft, S.L., Brun, R., Nwaka, S., 2004. Antimalarial drug discovery: efficacy models for compound screening. Nat. Rev. Drug Discov. 3, 509–520. https://doi.org/10.1038/nrd1416.

Fivelman, Q.L., Adagu, I.S., Warhurst, D.C., 2004. Modified fixed-ratio isobologram method for studying in vitro interactions between atovaquone and proguanil or dihydroartemisinin against drug-resistant strains of Plasmodium falciparum. Antimicrob. Agents Chemother. 48, 4097–4102. https://doi.org/10.1128/AAC.48.11.4097-4102.2004.

Fujimoto, Y., Agusutein, S., Made, S., 1987. Isolation of a Chalcone Derivative and Antitumor Compositions Containing it. (Japan Patent No. JP 86-50070 19860307).

Fujimoto, Y., Koshihara, Y., Made, S., Agusutein, S., 1988. Isolation of 2-Geranyl-3,4,2',4'- Tetrahydroxychalcone as an Antiallergy Agent. (Japan Patent No. JP 86-167288 19860716).

Gomes, M., Muratov, E., Pereira, M., Peixoto, J., Rosseto, L., Cravo, P., Andrade, C., Neves, B., 2017. Chalcone derivatives: promising starting points for drug design. Molecules 22, 1210. https://doi.org/10.3390/molecules22081210.

Goodman, C.D., Buchanan, H.D., McFadden, G.I., 2017. Is the mitochondrion a good malaria drug target? Trends Parasitol. 33, 185–193. https://doi.org/10.1016/j.pt.2016.10.002.

Hafid, A.F., Ariantari, N.P., Tumewu, L., Widyawaruyanti, A.R.H.A., 2012. The active marker compound identification of Artocarpus champeden Spreng. stembark extract, morachalchone a as antimalarial. Int. J. Pharm. Pharmaceut. Sci. 4, 246–249.

Hafid, A.F., Septiani, R.P., Febrianty, L.H.F.N., Ranggaditya, D., Widyawaruyanti, A., 2016. Antimalarial activity of crude extracts of Artocarpus heterophyllus, Artocarpus altilis, and Artocarpus camansi. Asian J. Pharmaceut. Clin. Res. 9, 261–263.

Hakim, E.H., Achmad, S.A., Juliawaty, L.D., Makmur, L., Syah, Y.M., Aimi, N., Kitajima, M., Takayama, H., Ghisalberti, E.L., 2006. Prenylated flavonoids and related compounds of the Indonesian Artocarpus (Moraceae). J. Nat. Med. 60, 161–184. https://doi.org/10.1007/s11418-006-0048-0.

Hartuti, E.D., Inaoka, D.K., Komatsuya, K., Miyazaki, Y., Miller, R.J., Xinying, W., Sadikin, M., Prabandari, E.E., Waluyo, D., Kuroda, M., Amalia, E., Matsuo, Y., Nugroho, N.B., Saimoto, H., Pramisandi, A., Watanabe, Y.-I., Mori, M., Shiomi, K., Balogun, E.O., Shiba, T., Harada, S., Nozaki, T., Kita, K., 2018. Biochemical studies of membrane bound Plasmodium falciparum mitochondrial L-malate:quinone oxidoreductase, a potential drug target. Biochim. Biophys. Acta - Bioenerg. 1859, 191–200. https://doi.org/10.1016/j.bbabio.2017.12.004.

Heyne, K., 1987. The Useful Indonesian Plants (B. L. K. Jakarta, Trans.). Research and Development Agency.

Hidayati, A.R., Widyawaruyanti, A., Ilmi, H., Tanjung, M., Widiandani, T., Siswandono, S.S., Syafruddin, D., Hafid, A.F., 2020. Antimalarial activity of flavonoid compound isolated from leaves of artocarpus altilis. Pharmacogn. J. 12, 835–842. https://doi.org/10.5530/pj.2020.12.120.

Hino, A., Hirai, M., Tanaka, T.Q., Watanabe, Y.I., Matsuoka, H., Kita, K., 2012. Critical roles of the mitochondrial complex II in oocyst formation of rodent malaria parasite Plasmodium berghei. J. Biochem. 152, 259–268. https://doi.org/10.1093/jb/mvs058.

Hoppe, H.C., van Schalkwyk, D.A., Wiehart, U.I.M., Meredith, S.A., Egan, J., Weber, B. W., 2004. Antimalarial quinolines and artemisinin inhibit endocytosis in Plasmodium falciparum. Antimicrob. Agents Chemother. 48, 2370–2378. https://doi.org/10.1128/AAC.48.7.2370-2378.2004.

Inaoka, D.K., Komatsuya, M.E.O.B., Amalia, E., Saimoto, H., Kita, K., 2016. Functional Expression of Mitochondrial Malate: quinone oxidoreductase from Plasmodium falciparum in bacterial membrane and identification of nanomolar inhibitor. In: International Congress for Tropical Medicine and Malaria. Brisbane (Australia).

Inaoka, D.K., Sakamoto, K., Shimizu, H., Shiba, T., Kurisu, G., Nara, T., Aoki, T., Kita, K., Harada, S., 2008. Structures of Trypanosoma cruzi dihydroorotate dehydrogenase complexed with substrates and products: atomic resolution insights into mechanisms of dihydroorotate oxidation and fumarate reduction. Biochemistry 47, 10881–10891. https://doi.org/10.1021/bi800413r.

Jagtap, U.B., Bapat, V.A., 2010. Artocarpus: a review of its traditional uses, phytochemistry and pharmacology. J. Ethnopharmacol. 129, 142–166. https://doi.org/10.1016/j.jep.2010.03.031.

Jayaraman, V., Bulusu, V., Balaram, H., 2012. Crosstalk between purine nucleotide metabolism and mitochondrial pathways in Plasmodium falciparum. Curr. Sci. 102, 757–766.

Jayasinghe, L., Balasooriya, B.A.I., Padmini, W.C., Hara, N., Fujimoto, Y., 2004. Geranyl chalcone derivatives with antifungal and radical scavenging properties from the leaves of Artocarpus nobilis. Phytochemistry 65, 1287–1290. https://doi.org/10.1016/j.phytochem.2004.03.033.

Ke, H., Ganesan, S.M., Dass, S., Morrisey, J.M., Pou, S., Nilsen, A., Riscoe, M.K., Mather, M.W., Vaidya, A.B., 2019. Mitochondrial type II NADH dehydrogenase of Plasmodium falciparum (PfNDH2) is dispensable in the asexual blood stages. PLoS One 14, e0214023. https://doi.org/10.1371/journal.pone.0214023.

Ke, H., Lewis, I.A., Morrisey, J.M., McLean, K.J., Ganesan, S.M., Painter, H.J., Mather, M. W., Jacobs-Lorena, M., Llinás, M., Vaidya, A.B., 2015. Genetic investigation of tricarboxylic acid metabolism during the Plasmodium falciparum Life Cycle. Cell Rep. 11, 164–174. https://doi.org/10.1016/j.celrep.2015.03.011.

Kochummen, K.M., 1982. In: Whitmore, T. (Ed.), Tree Flora of Malaya: A Manual for Foresters. Longman Malaysia.

Koshihara, Y., Fujimoto, Y., Inoue, H., 1988. A new 5-lipoxygenase selective inhibitor derived from Artocarpus communis strongly inhibits arachidonic acid-induced ear edema. Biochem. Pharmacol. 37, 2161–2165. https://doi.org/10.1016/0006-2952(88)90576-x.

Lambros, C., Vanderberg, J.P., 1979. Synchronization of Plasmodium falciparum erythrocytic stages in culture. J. Parasitol. 65, 418. https://doi.org/10.2307/3280287.

Lemmens, R.H.M.J., Soerianegara, I., Wong, W.C., 1995. Plant resources of south-east Asia. Timber trees: minor commercial timbers 5 (2). Backhuys Publishers.

Lianos-Cuentas, A., Casapia, M., Chuquiyauri, R., Hinojosa, J.-C., Kerr, N., Rosario, M., Toovey, S., Arch, R.H., Phillips, M.A., Rozenberg, F.D., Bath, J., Ng, C.L., Cowell, A. N., Winzeler, E.A., Fidock, D.A., Baker, M., Möhrle, J.J., Hooft van Huijsduijnen, R., Gobeau, N., Araeipour, N., Andenmatten, N., Rückle, T., Duparc, S., 2018. Antimalarial activity of single-dose DSM265, a novel plasmodium dihydroorotate dehydrogenase inhibitor, in patients with uncomplicated Plasmodium falciparum or Plasmodium vivax malaria infection: a proof-of-concept, open-label, phase 2a study. Lancet Infect. Dis. 18, 874–883. https://doi.org/10.1016/S1473-3099(18)30309-8.

McCarthy, J.S., Lotharius, J., Rückle, T., Chalon, S., Phillips, M.A., Elliott, S., Sekuloski, S., Griffin, P., Ng, C.L., Fidock, D.A., Marquart, L., Williams, N.S., Gobeau, N., Bebrevska, L., Rosario, M., Marsh, K., Möhrle, J.J., 2017. Safety, tolerability, pharmacokinetics, and activity of the novel long-acting antimalarial DSM265: a two-part first-in-human phase 1a/1b randomised study. Lancet Infect. Dis. 17, 626–635. https://doi.org/10.1016/S1473-3099(17)30171-8.

Mi-Ichi, F., 2005. Parasite mitochondria as a target of chemotherapy: inhibitory effect of licochalcone A on the plasmodium falciparum respiratory chain. Ann. N. Y. Acad. Sci. 1056, 46–54. https://doi.org/10.1196/annals.1352.037.

Miyazaki, Y., Inaoka, D.K., Shiba, T., Saimoto, H., Sakura, T., Amalia, E., Kido, Y., Sakai, C., Nakamura, M., Moore, A.L., Harada, S., Kita, K., 2018. Selective cytotoxicity of dihydroorotate dehydrogenase inhibitors to human cancer cells under hypoxia and nutrient-deprived conditions. Front. Pharmacol. 9 https://doi.org/10.3389/fphar.2018.00997.

Nakano, J., Uchida, K., 1990. Preparation of 2- Geranyl-3,4,2',4'-Tetrahydroxydihydrochalcone and its Intermediates. (Japan Patent No. JP 88-164577 19880630).

Niikura, M., Komatsuya, K., Inoue, S.-I., Matsuda, R., Asahi, H., Inaoka, D.K., Kita, K., Kobayashi, F., 2017. Suppression of experimental cerebral malaria by disruption of malate:quinone oxidoreductase. Malar. J. 16, 247. https://doi.org/10.1186/s12936-017-1898-5.

Painter, H.J., Morrisey, J.M., Mather, M.W., Vaidya, A.B., 2007. Specific role of mitochondrial electron transport in blood-stage Plasmodium falciparum. Nature 446, 88–91. https://doi.org/10.1038/nature05572.

Pan, W.-H., Xu, X.-Y., Shi, N., Tsang, S., Zhang, H.-J., 2018. Antimalarial activity of plant metabolites. Int. J. Mol. Sci. 19, 1382. https://doi.org/10.3390/ijms19051382.

Patil, A.D., Freyer, A.J., Killmer, L., Offen, P., Taylor, P.B., Votta, B.J., Johnson, R.K., 2002. A New dimeric dihydrochalcone and a new prenylated flavone from the bud covers of artocarpus a ltilis : potent inhibitors of cathepsin K. J. Nat. Prod. 65, 624–627. https://doi.org/10.1021/np0105634.

Perry, L.M., 1980. Medicinal Plants of East and Southeast Asia: Attributed Properties and Uses. MIT Press, Cambridge, Massachusetts.

Pink, R., Hudson, A., Mouriès, M.-A., Bendig, M., 2005. Opportunities and challenges in antiparasitic drug discovery. Nat. Rev. Drug Discov. 4, 727–740. https://doi.org/10.1038/nrd1824.

Reynolds, E.S., 1963. The use of lead citrate at high ph as an electron-opaque stain in electron microscopy. J. Cell Biol. 17, 208–212. https://doi.org/10.1083/jcb.17.1.208.

Ruan, J., Li, Z., Zhang, Ying, Chen, Y., Liu, M., Han, L., Zhang, Yi, Wang, T., 2019. Bioactive constituents from the roots of eurycoma longifolia. Molecules 24. https://doi.org/10.3390/molecules24173157.

Sachanonta, N., Chotivanich, K., Chaisri, U., Turner, G.D.H., Ferguson, D.J.P., Day, N.P. J., Pongponratn, E., 2011. Ultrastructural and real-time microscopic changes in P. falciparum -infected red blood cells following treatment with antimalarial drugs. Ultrastruct. Pathol. 35, 214–225. https://doi.org/10.3109/01913123.2011.601405.

Saxena, S., Neerja Pant, D.C.J., Bhakuni, R.S., 2003. Antimalarial agents from plant sources. Curr. Sci. 85, 1314–1329.

Shimizu, K., Kondo, R., Sakai, K., Buabarn, S., Dilokkunanant, U., 2000. 5α-Reductase inhibitory component from leaves of Artocarpus altilis. J. Wood Sci. 46, 385–389. https://doi.org/10.1007/BF00776401.

Sikarwar, M.S., Hui, B.J., Subramaniam, K., Valeisamy, B.D., 2014. A review on artocarpus altilis (Parkinson) Fosberg (breadfruit). J. Appl. Pharmaceut. Sci. 4, 91–97.

Siregar, J.E., Kurisu, G., Kobayashi, T., Matsuzaki, M., Sakamoto, K., Mi-ichi, F., Watanabe, Y., Hirai, M., Matsuoka, H., Syafruddin, D., Marzuki, S., Kita, K., 2015. Direct evidence for the atovaquone action on the Plasmodium cytochrome bc 1 complex. Parasitol. Int. 64, 295–300. https://doi.org/10.1016/j.parint.2014.09.011.

Somashekhar, M., Nayeem, N., Sonnad, B., 2013. A review on family Moraceae (Mulberry) with a focus on artocarpus species. World J. Pharm. Pharmaceut. Sci. 2, 2614–2626.

Syah, Y.M., Acmad, S.A., Bakhtiar, E., Hakim, E.H., Juliawaty, L.D., Latip, J., 2006. Dua flavonoid Tergeranilasi Dari Daun Sukun (artocarpus altilis). J. Mat. dan Sains 11.

Takac, P., Kello, M., Pilatova, M.B., Kudlickova, Z., Vilkova, M., Slepcikova, P., Petik, P., Mojzis, J., 2018. New chalcone derivative exhibits antiproliferative potential by inducing G2/M cell cycle arrest, mitochondrial-mediated apoptosis and modulation of MAPK signalling pathway. Chem. Biol. Interact. 292, 37–49. https://doi.org/10.1016/j.cbi.2018.07.005.

Trager, W., Jensen, J.B., 1976. Human malaria parasites in continuous culture. Science (80-.) 193, 673–675. https://doi.org/10.1126/science.781840.

Verheij, E.W.M., Coronel, R.E., 1992. Plant Resources of South-East Asia. No. 2: Edible Fruits and Nuts. Wageningen (Netherlands) Pudoc.

Wang, X., Miyazaki, Y., Inaoka, D.K., Hartuti, E.D., Watanabe, Y.-I., Shiba, T., Harada, S., Saimoto, H., Burrows, J.N., Benito, F.J.G., Nozaki, T., Kita, K., 2019. Identification of Plasmodium falciparum mitochondrial malate: quinone oxidoreductase inhibitors from the pathogen box. Genes (Basel) 10, 471. https://doi.org/10.3390/genes10060471.

WHO, 2020. World malaria Report 2020 [WWW Document]. URL. https://www.who.int/docs/default-source/malaria/world-malaria-reports/9789240015791-double-page-view.pdf?sfvrsn=2c24349d_5.

Widyawaruyanti, A., Subehan, Kalauni, S.K., Awale, S., Nindatu, M., Zaini, N.C., Syafruddin, D., Asih, P.B.S., Tezuka, Y., Kadota, S., 2007. New prenylated flavones from Artocarpus champeden, and their antimalarial activity in vitro. J. Nat. Med. 61, 410–413. https://doi.org/10.1007/s11418-007-0153-8.

Wunderlich, J., Rohrbach, P., Dalton, J.P., 2012. The malaria digestive vacuole. Front. Biosci. (Schol. Ed). 4, 1424–1448. https://doi.org/10.2741/s344.

Yamashita, T., Inaoka, D.K., Shiba, T., Oohashi, T., Iwata, S., Yagi, T., Kosaka, H., Miyoshi, H., Harada, S., Kita, K., Hirano, K., 2018. Ubiquinone binding site of yeast NADH dehydrogenase revealed by structures binding novel competitive- and mixed-type inhibitors. Sci. Rep. 8, 2427. https://doi.org/10.1038/s41598-018-20775-6.

Yayon, A., Timberg, R., Friedman, S., Ginsburg, H., 1984. Effects of chloroquine on the feeding mechanism of the intraerythrocytic human malarial parasite Plasmodium falciparum. J. Protozool. 31, 367–372. https://doi.org/10.1111/j.1550-7408.1984.tb02981.x.